

Collective Plasmonic-Molecular Modes in the Strong Coupling Regime

Adi Salomon,¹ Robert J. Gordon,² Yehiam Prior,¹ Tamar Seideman,³ and Maxim Sukharev⁴

¹*Chemical Physics Department, Weizmann Institute of Science, 76100 Rehovot, Israel*

²*Department of Chemistry, University of Illinois at Chicago,*

845 W Taylor Street, Chicago, IL 60680, USA

³*Department of Chemistry, Northwestern University,*

2145 Sheridan Road, Evanston, IL 60208, USA

⁴*Department of Applied Sciences and Mathematics,*

Arizona State University, Mesa, Arizona 85212, USA

(Dated: December 2, 2024)

We demonstrate strong coupling between molecular excited states and surface plasmon modes of a slit array in a thin metal film. The coupling manifests itself as an anti-crossing behavior of the two newly formed polaritons. At stronger coupling a new mode emerges that is due to long range molecular interactions mediated by the plasmonic field. The new molecular-like mode repels the polariton states, and leads to an opening of energy gaps on both sides.

PACS numbers: PCS

INTRODUCTION

The emerging field of nano-plasmonics opened up new possibilities for the study of light-matter interactions at the nano scale, especially when molecules are placed in the regions where the electromagnetic fields are both enhanced and focused to nano scale area by plasmonic resonances [1–3] Systems comprised of metallic nanostructured arrays are particularly attractive for interaction with photonic molecular excited states, as the plasmonic resonances may be tuned by geometrical factors (e.g., the periodicity of arrays) to exactly match the molecular frequencies [4]. Indeed, strong Interactions between plasmonic and molecular modes have been observed in recent years both for localized [5–8] and delocalized [9–14] plasmonic modes. The interaction of molecules with surface plasmons is similar to that

in microcavities [15–18], where the cavity modes dispersion relations are replaced by the plasmonic ones. In the strong coupling regime, energy exchange between the molecular and plasmonic modes is observed, giving rise to two new polariton eigenmodes. The strong coupling manifests itself as an avoided crossing of the polariton modes as a function of the plasmon frequency, with an observed Rabi splitting (RS) which is a non-negligible fraction of the molecular transition frequency [7, 10, 11, 19, 20]. In some experimental studies, but not in others even when strong coupling is clearly present, a new spectral feature was observed near the molecular transition, but its nature requires further study [7, 11, 21]

Here we study the interaction between plasmonic modes excited within an array of slits in a thin silver film and with a layer of molecules deposited in close proximity to the surface. We use a self-consistent model and numerically solve the Maxwell-Liouville-von Neumann equations, where the coupling between the molecular excitations and the metallic surface plasmon (SP) modes is explicitly taken into account. In addition to providing a detailed analysis of the origin of the avoided crossing between the split resonance components as the array spacing varies, we report on the emergence of a new mode. The spectral properties of the new mode are different from those of both the surface plasmon polariton (SPP) and the molecular modes that led to its onset. We simulate the SPP-molecular interaction in this strong coupling regime for experimentally realizable parameters and explore its dependence on the dipole strength, the molecular density, and the distance of the molecular layer from the surface. We illustrate the conditions under which such new spectral features are expected, and unravel their signatures of the strong coupling regime in the new context of nanoplasmonics. The strong coupling regime is further characterized by a new asymptotic energy gap between the SPP modes and the molecular spectral position, a phenomenon that is directly related to the existence of the new collective mode. In what follows we first describe the results, then elaborate our theoretical model, and finally conclude with a detailed discussion of our observations.

MODEL

Consider an infinite array of slits in a thin, 100nm, silver film shown in the inset in Fig. 1. The plasmonic response of this slit array may be tuned by adjusting the array periodicity [22]. For each periodicity, the transmission spectrum is calculated and the plasmonic peak

position is derived. A 10nm molecular layer with its first electronic excited state lying at 2.62 eV above the ground state is placed above the silver slit array, with or without a spacer layer (see below). The silver dispersion relation is described by the conventional Drude model [23]. The hybrid system is illuminated from above by a white light continuum, and we calculate the transmission and reflection spectra. We restrict our treatment to two dimensions and consider only a transverse-electric (TE) incoming plane wave, with its electric field along the x-direction, with the assumption that characteristic cross-sectional geometrical parameters are independent of the y-coordinate (see the inset in Fig. 1). To model the molecular subsystem, we employ a self-consistent approach based on numerical integrations of the coupled Maxwell-Liouville-von Neumann equations. In order to take into account all possible electric field polarizations in the near-field zone, the molecular layer is modeled as a three-level quantum system with two degenerate excited states representing the p_x and p_z orbitals. We adopt the numerical implementation and methodology discussed in details in Ref. [24]. In brief, in spatial regions occupied by molecules we numerically integrate the relevant Maxwell-Liouville-von Neumann equations and evaluate the macroscopic polarization of the combined molecular-plasmonic ensemble. The time derivative of the latter is used as a source in Amperes law. The electrodynamics of the hybrid system is treated by a finite-difference time-domain algorithm [25]. The resulting system of equations is solved numerically on a local cluster [26]. For the uncoupled system, the molecular line and the bare SP spectrum (for 160 nm wide slits, at a periodicity of 410 nm) are depicted in Fig. 1. As noted, by changing the array periodicity we can scan the SP resonance frequency.

At first the hybrid system is studied at low molecular density, where the molecular dipole-dipole interaction is small, and the electromagnetic field (external and locally generated) may be assumed to interact individually with each molecule. A set of transmission spectra of the hybrid system, over the relevant energy range and for different array periodicities, is displayed in Fig. 2a. The system parameters (see the legend of Fig. 2) were chosen such that the SP mode and the molecular mode can be easily distinguished by their different line-widths. As the array periodicity is tuned, a clear picture of avoided-crossing is observed, both in Fig. 2a, where the actual spectra are shown, and in Fig. 2b, where the peak position of the upper and lower polaritons, E_u and E_l , are plotted as a function of the array wave-vector ($k = 2\pi/\text{periodicity}$). At shorter periods, the upper polariton (blue curve) is plasmonic in nature (having a broad spectral line due to short life time). As the

periodicity is scanned through the molecular resonance, this polariton changes its character and becomes molecular in nature (narrow line). The lower polariton follows the opposite path. At 410 nm periodicity, the two polaritons anti-cross, with a Rabi splitting of 35 meV, reflecting the coupling strength of the molecular-plasmon interaction for the parameters used in this calculation. The solid curves superimposed on the numerically derived anti-crossing eigenmodes are the result of diagonalizing the (2x2) diabatic Hamiltonian,

$$H = \begin{pmatrix} E_m & \Delta \\ \Delta & E_{pl}(k) \end{pmatrix}, \quad (1)$$

where RS is $2\Delta = 35$ meV and $E_{pl}(k)$ are SP modes derived from our simulations in the absence of molecules. Thus, the dispersion relation for the newly formed polaritons is given by [15, 16]

$$E_{u,l}(k) = \frac{E_{pl}(k) + E_m}{2} \pm \sqrt{\Delta^2 + \frac{(E_{pl}(k) - E_m)^2}{4}}. \quad (2)$$

This model corresponds to the interaction of isolated molecules with the plasmonic modes. While its main predictions are verified experimentally, the model is not expected to be valid for high molecular densities or for strong inter-molecular interactions. Moreover, this simple model is stationary, and therefore it is unable to provide information about the lifetime and the emission spectrum of the coupled system [27].

As the molecular density increases, intermolecular dipole-dipole forces and in particular polariton mediated molecular coupling, grow significantly, and the two-level model presented above becomes invalid. Fig.3a depicts a series of transmission spectra for different molecular densities, ranging from 10^{23} molecules/m³ (corresponding to an average intermolecular distance of 50 nm) to 10^{26} molecules/m³ (with the average intermolecular distance of 5 nm). The inset depicts the RS values at resonance as a function of the molecular density. At low densities, the two-level model fits the data well, and the RS values are proportional to the square root of the molecular density [15, 16]. At the higher densities, when the intermolecular distance approaches a few nanometers, a new peak appears in the transmission spectrum near the molecular frequency, and deviations are observed in the density dependence of the RS splitting.

A similar role is played by the magnitude of the dipole moment, which likewise controls the intermolecular interaction strength. Fig. 3b shows a series of transmission plots for different dipole moment magnitudes, illustrating that both the RS values and the appearance on the

new mode are strongly dependent on the molecular dipole moment. The inset shows a linear dependence of the RS on the dipole moment (see below).

Next, we repeat the type of calculation that led to Fig. 2, namely the transmission spectrum as a function of array periodicity, but this time for a much higher molecular density. Thus, unlike the previous case, where the EM field interacted with individual molecules, here, because of the closer proximity of the molecules, the inter-molecule interactions are enhanced, and collective behavior of the entire molecular ensemble is observed as is shown in Fig. 4. Fig. 4a depicts a series of spectra where the avoided crossing and the extra peak are clearly visible, and Fig. 4b shows the peak positions extracted from the calculations. In Fig. 4b, the two polaritons repel each other further, leading to an observed RS of 150 meV, and the emergence of a new peak. The new mode is only slightly dispersive and stays close to the molecular transition frequency as the SP modes are tuned, something that indicates its molecular character rather than a plasmonic one. Another new feature is now clearly seen. Whereas at small coupling strength (i.e. the conditions of Fig. 2), both the upper and the lower polaritons approach asymptotically (far from resonance) the molecular transition energy, here the behavior is different. The upper polariton opens up an energy gap, and asymptotically tends to a value that is higher than the molecular transition energy by 70 meV, a very large fraction of the observed RS splitting of 150 meV. Likewise, the lower polariton also develops an energy gap, albeit smaller (15 meV). As discussed below, these energy gaps are closely related to the appearance of the new collective peak and serve as another signature of strong coupling.

To further elucidate the origin of the new observations, we proceed to insert a spacer layer with a refractive index of one and with varying thickness between the molecules and the silver film the purpose here is to check the dependence of the intermolecular coupling on the strength of the plasmonic field, which decays exponentially with distance from the surface. Fig. 5 is a 3-dimensional plot depicting transmission spectra for a series of distances, ranging from a few nm, where the plasmonic interaction is full, to a distance of 300 nm, where the interaction is negligible due to the exponential decay of the SP modes. Two observations are noted; first, the new mode peak position is intense not only at close proximity to the metal layer but also at distances of 50 nm and 100 nm. Yet, as the spacer thickness increases it gradually merges with the upper polariton and disappears. Second, the RS separation between the two polaritons decreases exponentially, as expected due to the decay nature of

the plasmonic field. The decay of the collective mode with the decrease of the plasmonic field, as is seen in Fig. 5, provides further support to the dependence of this mode on plasmon-mediated dipole-dipole coupling.

The electrostatic interaction energy between two dipoles interacting in free space is inversely proportional to the third power of the distance between them. For molecules a few nm apart, this direct interaction is small and is neglected in our calculations. However, because the molecules are immersed in the strong polaritonic field in a two-dimensional thin layer near the surface, they are subject to a different type of coupling. The molecules are still coupled through their dipole moments (hence the dependence on the dipole moment value), but the relevant fields responsible for the coupling are the propagating polaritons. Plasmon-mediated dipole-dipole interactions are qualitatively and quantitatively different from the interaction through free space. Unlike free space, where the electrostatic interaction spreads in all directions, here the interaction takes place in a space of reduced dimensionality. Dipolar interactions in reduced dimensions have been discussed before, near nanoparticles and in wave-guides [28, 29], and were shown to give rise to efficient coupling. Here the dipoles lie in a two-dimensional layer, but the plasmon propagation is not isotropic in this 2D space, and the coupling is therefore expected to be an intermediate case between one and two dimensions. In this restricted lower dimensional space, the inverse distance dependence of the interaction is expected to be lower than third power. Thus, for shorter distances (higher densities) the interaction energy is higher than for the three dimensional free space. The full analysis of this coupling will be the subject of a future publication.

CONCLUSION

In conclusion, the self-consistent solution to the Maxwell-Liouville-von Neumann equations provides new insights for the strong coupling regime between molecules and SP modes. We show that at high molecular densities, a plasmon-mediated inter-molecule coupling mechanism exists, which gives rise to a new collective mode of the molecular system, the origin of which is clarified here for the first time. The collective mode results from long-range, plasmon-mediated molecular interactions and is expected in other systems, where molecules interact strongly with propagating plasmons. The mechanism leading to the collective behavior gives rise to the new mode and causes a repulsion of the upper polariton and the

appearance of a new energy gap.

Although a simple model sufficed to explain the mode structure, the observed phenomena are general and are expected to play a role in many realistic systems with strong interaction between surface plasmons and molecular ensembles. Our model provides tools for tuning the properties of hybrid materials (molecules interacting with a plasmonic array), for applications in areas such as photochemistry and optical device engineering. In addition to using the periodicity of the nano-slit array to modify its optical properties, it may also be possible to design optimal electromagnetic fields to control the plasmon-molecule coupling. For example, a strong pre-pulse might be used to create a transient change in the refractive index of the array, and shaping of the spectral phase of a probe pulse could be used to control the coupling strength. Better understanding of the properties of mixed plasmon-molecule states may open up the potential for engineering non-linear optical devices.

-
- [1] E. M. Purcell, *Phys. Rev.* **69**, 681, (1946).
 - [2] A. Nitzan, and L. E. Brus, *J. Chem. Phys.* **75**, 2205, (1981).
 - [3] W. L. Barnes, *J. Mod. Optic.* **45**, 661, (1998).
 - [4] L. Martn-Moreno et al., *Phys. Rev. Lett.* **86**, 1114, (2001).
 - [5] N. I. Cade et al., *Phys. Rev. B* **79**, (2009).
 - [6] A. Biesso et al., *J. Am. Chem. Soc.* **131**, 2442, (2009).
 - [7] Y. Sugawara et al., *Phys. Rev. Lett.* **97**, (2006).
 - [8] M. Ringler et al., *Phys. Rev. Lett.* **100**, 203002, (2008).
 - [9] J. Bellesa et al., *Phys. Rev. Lett.* **93**, 036404, (2004).
 - [10] J. Dintinger et al., *Phys. Rev. B* **71**, 035424, (2005).
 - [11] A. Salomon et al., *Angew. Chem. Int. Ed.* **48**, 8748, (2009).
 - [12] A. Berrier et al., *ACS Nano* **5**, 6226, (2011).
 - [13] D. E. Gomez et al., *Nano Lett.* **10**, 274, (2010).
 - [14] G. P. Wiederrecht et al., *Phys. Rev. Lett.* **98**, 083001, (2007).
 - [15] V. M. Agranovich et al., *Phys. Rev. B* **67**, 085311, (2003).
 - [16] D. G. Lidzey et al., *Nature* **395**, 53, (1998).
 - [17] H. Yokoyama et al., *Appl. Phys. Lett.* **57**, 2814, (1990).

- [18] M. Bayer, *Phys. Rev. Lett.* **86**, 3168, (2001).
- [19] T. Schwartz et al., *Phys. Rev. Lett.* **106**, (2011).
- [20] T. K. Hakala et al., *Phys. Rev. Lett.* **103**, 053602, (2009).
- [21] J. A. Hutchison et al., *Angew. Chem. Int. Edit.* **50**, 2085, (2011).
- [22] T. W. Ebbesen et al., *Nature* **391**, 667, (1998).
- [23] L. Novotny, and S. J. Stranick, *Annu Rev. Phys. Chem.* **57**, 303, (2006).
- [24] M. Sukharev, and A. Nitzan, *Phys. Rev. A* **84**, 043802, (2011).
- [25] A. Taflove and S. C. Hagness, *Computational electrodynamics: the finite-difference time-domain method*, 3rd ed. (Artech House, Boston, 2005).
- [26] <http://plasmon.poly.asu.edu>
- [27] A. Trgler, and U. Hohenester, *Phys. Rev. B* **77**, 115403, (2008).
- [28] D. Martin-Cano et al., *Nano Lett.* **10**, 3129, (2010).
- [29] V. N. Pustovit, and T. V. Shahbazyan, *Phys. Rev. Lett.* **102**, (2009).

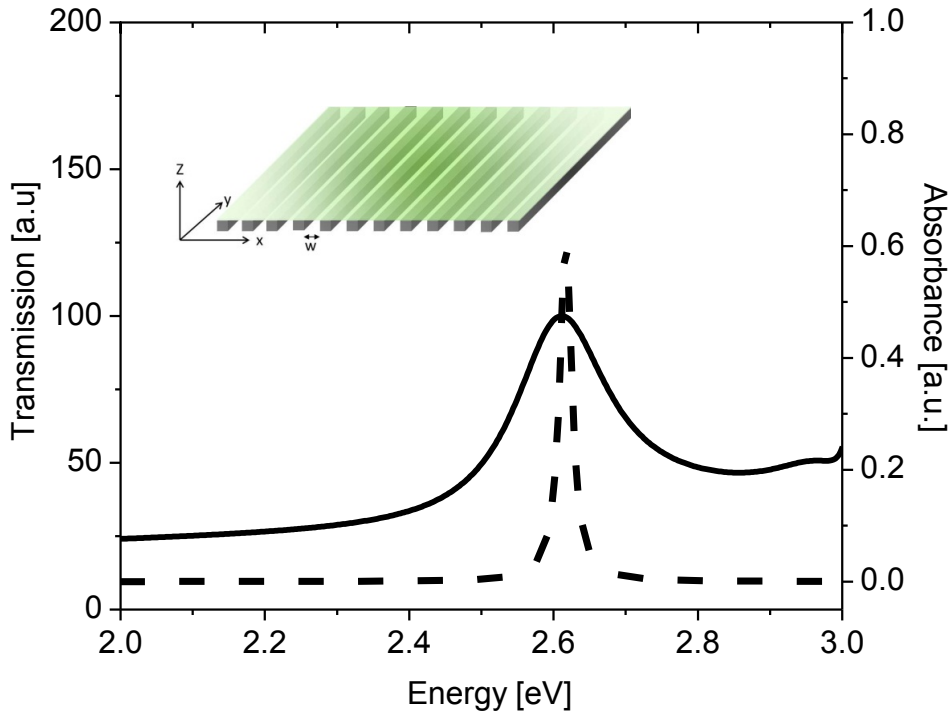


FIG. 1: (Color online). The simulated absorption spectrum (dash line) of a 10nm molecular layer and transmission spectrum (solid line) of bare Ag slit array. The molecular subsystem has the following parameters: transition frequency is 2.616 eV, transition dipole moment is 25.5 Debye, radiationless lifetime is 1 ps, and molecular density is $3 \times 10^{25} \text{ m}^{-3}$. The geometrical parameters of the slit array are: slit size of 160 nm, Ag thickness of 100 nm, and periodicity of 410 nm. The inset schematically depicts the hybrid system: molecular layer is deposited directly on the Ag slit array.

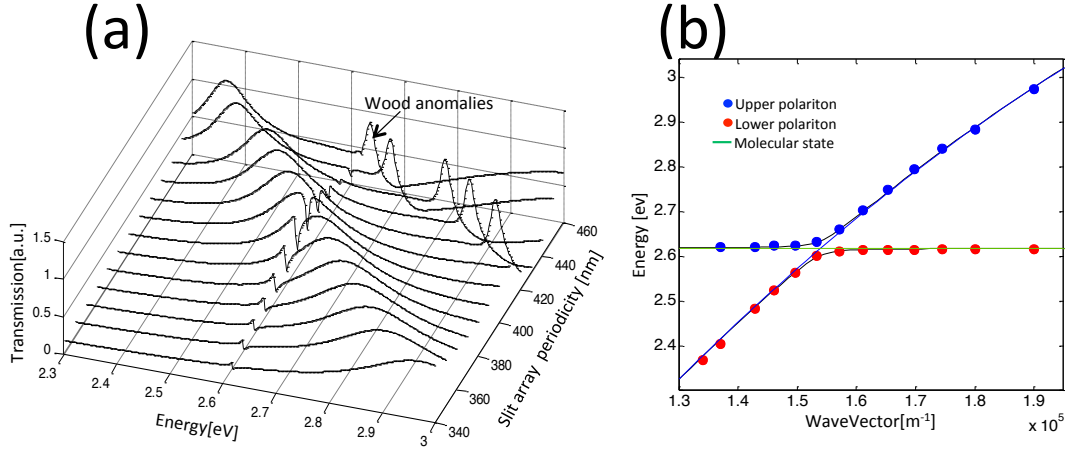


FIG. 2: (Color online). (a) Transmission spectra for the series of Ag slit arrays covered by a 10nm thin film of molecular layer with a density of 10^{24} m^{-3} . The molecular parameters are as for Fig. 1, but with radiationless lifetime of 300 fs. By changing the slit array periodicity, the SP modes are tuned to be off and on resonance with respect to the molecular subsystem. At the resonance a symmetric splitting is 30 meV. At large detuning value (period of 360 nm and 440 nm), the spectrum of the uncoupled modes is observed. (b) Positions of the peaks in the panel (a) are plotted as functions of the slit array period. The blue and the red circles correspond to the eigenstates of the system; the lower polaritons (red circles) and upper polaritons (blue circles).

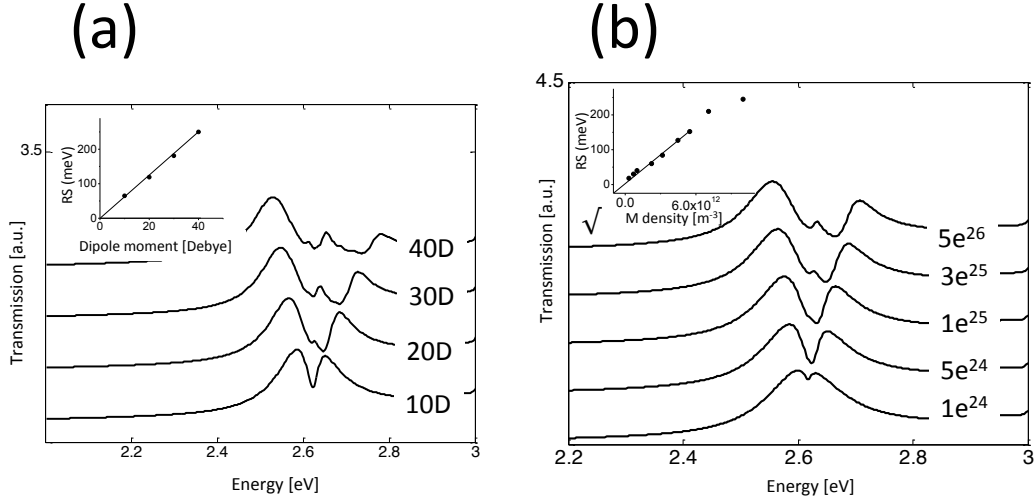


FIG. 3: (a) Transmission spectra for the Ag slit array with periodicity of 410nm, covered by a thin film of molecular layer with varied density. The molecular parameters are as for Fig. 1. When the molecular density is high, additional mode (splitting) is observed. The curves are shifted for clarity. Inset: RS values as function of the square root of the molecular densities. At low densities the RS scales linearly with the square root of the density and it fits to the classical model. (b) Same as in panel (a) but with varied transition dipole moment. An additional mode (splitting) is observed. The molecular density for all the simulated spectra is $3 \times 10^{25} \text{ m}^{-3}$. The curves are shifted for clarity. Inset: RS values as function of the molecular dipole moment values.

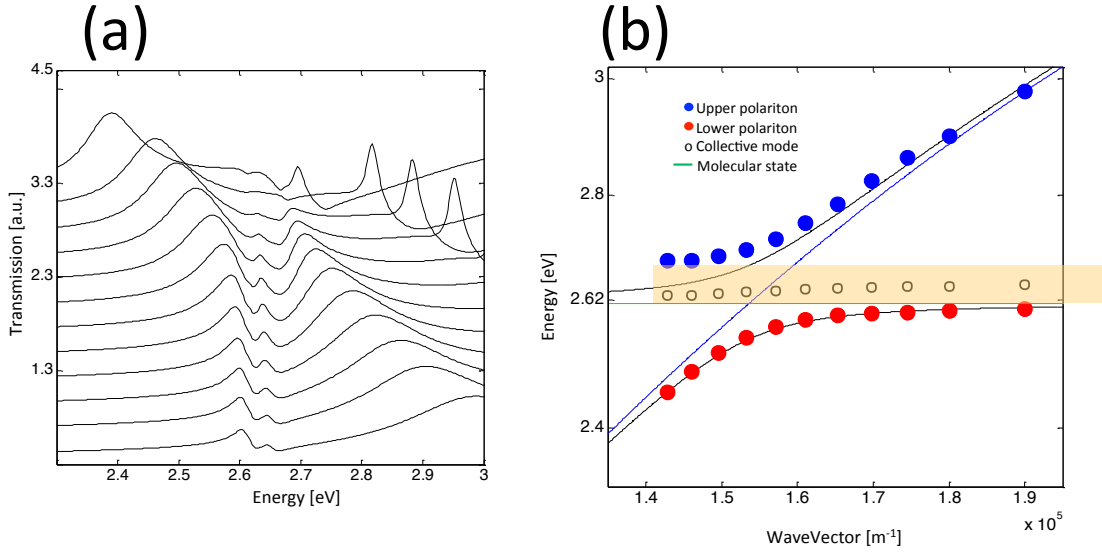


FIG. 4: (Color online). (a) The Same as in Fig. 2a but for higher molecular density of $3 \times 10^{25} \text{ m}^{-3}$ molecular density. An additional mode is clearly seen at about 2.64 eV. At large detuning value, there is a small shift of the original modes. The molecular subsystem has the following parameters: transition frequency is 2.616 eV, transition dipole moment is 25.5 Debye, radiationless lifetime is 1 ps, pure dephasing time is 100 fs. (b) Anti-crossing of the hybrid modes at RS value of 0.15 meV. The peak position of the additional mode does not change with detuning of the SP mode. The orange zone indicates the energy gap.

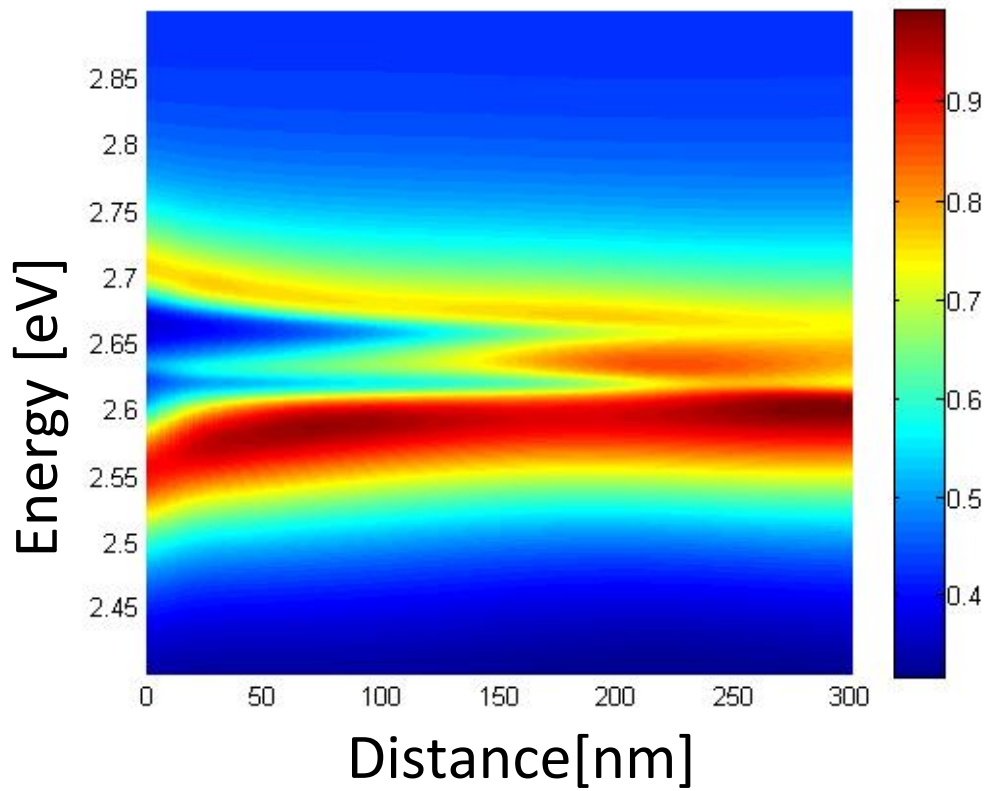


FIG. 5: (Color online). Transmission spectra for the Ag slit array with slit width of 160nm and periodicity of 410 nm covered by a spacer of $d = 0 - 300$ nm and a thin molecular film with the same parameters as for Fig1. At $d = 0 - 100$ nm 3 peaks are observed, whereas at $d = 300$ nm, the three peaks merges and almost no splitting is observed.